**Science and Technology Indonesia**
*e*-ISSN:2580-4391 *p*-ISSN:2580-4405
Vol. 10, No. 1, January 2025

Research Paper

# Stability of Biologically Synthesized Silver Nanoparticles (AgNPs) Using *Acalypha indica* L. Plant Extract as Bioreductor and Their Potential as Anticancer Agents Against T47D Cells

Luailik Madaniyah[1], Saidun Fiddaroini[1], Elok Kamilah Hayati[2], Moh. Farid Rahman[1], Akhmad Sabarudin[1,3*]

[1]*Department of Chemistry, Faculty of Science, Brawijaya University, Malang, 65145, Indonesia*
[2]*Chemistry Study Program, Faculty of Science and Technology, Maulana Malik Ibrahim Islamic State University, Malang, 65144, Indonesia*
[3]*Research Center for Advanced System and Material Technology, Brawijaya University, Malang, 65145, Indonesia*
***Corresponding author**: sabarjpn@ub.ac.id

**Abstract**
This work investigates the anticancer potential of silver nanoparticles (AgNPs) against T47D cells as well as the stability of AgNPs manufactured using extract from *Acalypha indica* L. used as a bioreductant. The plant extract was used to produce and stabilize AgNPs, and stability was tracked for 30 days using UV-Vis spectroscopy and Particle Size Analysis (PSA), which included evaluations of extended sun exposure. Transmission Electron Microscopy (TEM) was used to characterize the size and shape of the nanoparticles, and Fourier Transform-Infrared Spectroscopy (FT-IR) was used to determine which functional groups were responsible for stabilization. Despite a gradual size increase, the AgNPs remained stable throughout the study period. The MTT assay confirmed their potent cytotoxicity against T47D cells, underscoring the potential of *Acalypha indica*-derived AgNPs as stable and effective agents for cancer therapy, offering a promising alternative for novel anticancer treatments.

**Keywords**
Nanoparticle, *Acalypha indica* L., Plant Extract, Anticancer, Breast Cancer Cells

Received: 4 August 2024, Accepted: 25 October 2024
https://doi.org/10.26554/sti.2025.10.1.101-110

## 1. INTRODUCTION

Cancer is a malignant disease caused by the uncontrolled growth of cells in the body (Calcaterra et al., 2020). It ranks as the leading cause of death globally, significantly impacting life expectancy (Sung et al., 2021). As reported by the World Health Organization (2020), cancer ranks as the leading or second leading cause of premature death before the age of 70 in 112 out of 183 countries. In 2024, breast cancer is the most commonly diagnosed cancer among women in the United States, representing about 310,720 new cases, or 32% of all new cancer diagnoses. It ranks second in cancer-related mortality, following lung cancer, with 42,250 deaths (15% of all cancer deaths) (Siegel et al., 2024). In the last decade (2012-2019), the incidence of breast cancer increased more rapidly among women under 50 years old (1.1% per year) compared to those over 50 years old (0.5% per year). In Indonesia, WHO reported in 2020 that breast cancer ranked the highest, with a 16.6% risk among the population of 273 million (Nindrea et al., 2023).

The management of cancer is crucial to inhibit the mutation of abnormal cells. Standard cancer treatments include surgery, hormone therapy, immunotherapy, radiation therapy, and chemotherapy. These approaches are costly and come with side effects. The adverse effects of radiotherapy and surgery can damage healthy tissues surrounding the affected area, leading to long-term complications such as organ damage, skin abnormalities, or cardiovascular complications that can impact patients' well-being and hinder their capacity to carry out daily tasks (Belzile-Dugas and Eisenberg, 2021). Additionally, cancer drugs like doxorubicin, approved by the FDA, are often used in combination with other chemotherapy treatments (Sritharan and Sivalingam, 2021). However, chemical drugs can also damage normal cells and are often specific to certain cancer types.

Several studies on anticancer effects have utilized plant extracts from both terrestrial and marine sources (Basak et al., 2018; El-Refai et al., 2018; Heidari et al., 2018; Rahman et al., 2018, 2023), but their effectiveness needs improvement. Thus, novel advancements, such as drugs developed at the nanoscale, are needed to tackle chronic conditions like cancer (Yesilot and Aydın Acar, 2019). Nanoparticles are characterized as particles with dimensions ranging from 1 to 100 nanometers. Their unique physical properties, such as plasmon resonance

and enhanced fluorescence, as well as chemical properties like increased catalytic activity, are primarily influenced by their surface area-to-volume ratio and high reactivity (Chouhan, 2018), making them valuable for applications in anticancer therapy, antibacterial treatments, drug delivery, and various other health-related fields (Fiddaroini et al., 2023; Wulandari et al., 2022). As the diameter of spherical NPs decreases, the surface area increases proportionally, enhancing surface activity compared to larger dimensions (Xu et al., 2020). Despite the promise of nanotechnology, only a few nano products are viable for application due to unknown toxicity potential. Silver, a noble metal historically used for treatment and wound healing, is favored for its unique material properties, cost-effectiveness, and abundance in nature compared to other noble metals (Chen and Schluesener, 2008).

Metallic nanoparticles, including silver, gold, and platinum, have undergone extensive human testing. For their application in medicine, nanoparticles must be biocompatible and non-toxic or have low toxicity. The widely employed synthesis technique involves chemical reduction with reagents that reduce silver ions and stabilize nanoparticles. However, these reagents are toxic, pose health risks, and are also expensive (Guilger-Casagrande and Lima, 2019). Consequently, environmentally friendly biosynthesis methods are being developed, utilizing plants (Oves et al., 2022), bacteria (Ibrahim et al., 2019), fungi (Hamad, 2019), and algae (Naveenkumar et al., 2023) as bioreductors for silver nanoparticles.

Silver nanoparticles (AgNPs) demonstrate cytotoxic effects on cancer cells by modifying cell morphology, decreasing cell viability, and inducing oxidative stress (Aziz et al., 2019; Yoon et al., 2007). AgNPs are essential for tumor management due to their cytotoxic properties. Several plant species, such as *Gloriosa superba* L. tuber, have been employed in the biosynthesis of AgNPs to enhance their anticancer activity (Murugesan et al., 2021) and *Euphorbia prostate* (Dzoyem et al., 2022). *Artemisia turcomanica* leaf extract has been employed to synthesize AgNPs exhibit an average size of 22 nm, a Surface Plasmon Resonance (SPR) peak at 430 nm, and a face-centered cubic (fcc) crystal structure (Mousavi et al., 2018). Similarly, *Justica wynaadensis* leaf extract produced AgNPs sized 14-25 nm with an SPR peak at 445 nm and an fcc structure, exhibiting strong cytotoxicity against A549 cells with an $IC_{50}$ of 60 $\mu$g/mL (Lava et al., 2021). Additionally, AgNPs synthesized using *Olea europaea* extract demonstrated an SPR peak at 449 nm, particle sizes of 13-21 nm, and exhibited strong cytotoxicity against T47D cells ($IC_{50}$: 84 $\mu$g/mL) and weaker effects on MCF-7 cells ($IC_{50}$: $< 200$ $\mu$g/mL) (Felimban et al., 2022).

Stability of AgNPs refers to their ability to maintain physical, chemical, and functional properties over a specified period under defined storage conditions. This stability is essential for the efficacy and safety of AgNPs in medical, industrial, and environmental applications. Smaller nanoparticles tend to have higher surface activity, which may lead to aggregation during storage. This aggregation can alter particle size, diminish effectiveness, and affect optical properties such as color and absorbance. Storage conditions, including temperature, light, and humidity, significantly influence the stability of AgNPs. High temperatures can accelerate nanoparticle oxidation, while UV light exposure may cause changes in physical and chemical properties. Therefore, storage in dark conditions, at low temperatures, and in inert environments is recommended.

This study presents a new method for synthesizing silver nanoparticles (AgNPs) using *Acalypha indica* L. extract, emphasizing its environmentally friendly and sustainable nature. The research is focused on assessing the storage stability of biologically synthesized AgNPs under low-temperature and dark conditions to maintain their physical, chemical, and functional properties. The evaluation of AgNPs for their anticancer potential against T47D breast cancer cells demonstrates promising efficacy, providing insights into their therapeutic potential. Furthermore, the integration of in-silico analyses enhances our understanding of the molecular interactions involved, offering a comprehensive perspective on AgNPs as a viable alternative for cancer treatment. This study not only advances green nanotechnology but also paves the way for developing effective, stable, and targeted cancer treatments.

## 2. EXPERIMENTAL SECTION

### 2.1 Materials

The materials for this study were obtained from Merck and consist of *Acalypha indica* L. plant, distilled water ($H_2O$), and $AgNO_3$ (EMSURE 99%). A breast cancer cell line was acquired from the Animal Physiology, Structure, and Development Laboratory at the Department of Biology, Brawijaya University, and was kept in the Integrated Research Institute. The cells were grown in RPMI-1640 medium enriched with 1% Penicillin-Streptomycin and 10% Fetal Bovine Serum (FBS). The instruments used for material characterization included UV-Visible spectrophotometer (UV-Vis, Shimadzu 1601 Series), FTIR (Shimadzu 8400S), TEM (Hitachi TM 3000), Particle Size Analysis was conducted using a Zetasizer and ZS-explorer software, which utilized Dynamic Light Scattering (DLS) to assess the particle size distribution at 25°C. Anticancer activity assays were conducted using a microplate reader.

### 2.2 Preparation and Extraction of *Acalypha indica* L. Extract

The *Acalypha indica* L. plant was procured from Tuban and divided into its leaf, stem, and root components. These plant parts were thoroughly washed three times with tap water and twice with distilled water to eliminate any dirt and residues. The plant was then air-dried before being placed in an oven at 30°C until fully dried. Once dried, the plant was cut into small pieces, ground into a fine powder, and sieved through a 50-80 mesh screen. This powder was stored in a cool environment for further use. For extraction, 5 grams of the powdered *Acalypha indica* L. were combined with 200 mL of distilled water and boiled for 20 minutes at 60°C. After cooling, the solution was filtered using Whatman No.1 filter paper, and the resulting filtrate was stored at -4°C for future analysis.

### 2.3 Synthesis and Stability Testing of AgNPs

A 10 mL portion of *Acalypha indica* L. was mixed with 90 mL of 1 mM $AgNO_3$ in a conical flask. The solution was agitated using a magnetic stirrer for 10 minutes at room temperature. Once homogenized, the solution was exposed to sunlight with varying exposure times of 5, 10, and 20 minutes to promote the formation of AgNPs, as evidenced by a change in color. The optimal synthesis was determined based on UV-Vis spectra. Stability testing was conducted on days 0, 3, 7, 14, and 21, and was assessed using UV-Vis spectroscopy and Particle Size Analysis (PSA).

### 2.4 Anticancer Activity Assay Using MTT Method

T47D cells were grown in RPMI-1640 medium enriched with 10% Fetal Bovine Serum (FBS) and 1% penicillin-streptomycin. They were kept in a humidified incubator at 37°C with an atmosphere of 5% $CO_2$. The AgNPs were subjected to freeze-drying to achieve lyophilization. The lyophilized AgNPs were then individually reconstituted in 1% dimethyl sulfoxide (DMSO) to create stock solutions at a concentration of 1 mg/mL. These stock solutions were further diluted to obtain the final concentrations of 400, 200, 100, 50, and 25 $\mu$g/mL.

T47D cells were plated at a density of $1 \times 10^4$ cells/mL into 96-well plates and allowed to incubate for 24 hours. Subsequently, AgNPs were administered at concentrations of 400, 200, 150, 100, 50, and 25 $\mu$g/mL. Control wells, which received no treatment, and blank wells, which contained no cells, were included for comparison. After an additional 24-hour incubation, the medium was replaced with 100 $\mu$l of MTT solution and incubated for 3 hours. The resulting formazan crystals were then dissolved in DMSO, and absorbance was measured at 570 nm to assess cell viability. Cell viability was calculated using the following Equation (1):

$$\text{Cell viability}\ (\%) = \frac{(A-B)}{(C-B)} \times 100\% \qquad (1)$$

where ($A$) represents the sample absorbance, ($B$) denotes the blank absorbance, and ($C$) refers to the control absorbance. $IC_{50}$ values were calculated using Excel.

## 3. RESULT AND DISCUSSION

### 3.1 Synthesis of AgNPs Using *Acalypha indica* L. Plant Extract as a Bioreductor

The synthesis of AgNPs was conducted through a biological approach that utilizes bioreductors derived from compounds found in the *Acalypha indica* L. plant. During the extraction process using water as a solvent, the primary components identified in the extract include acalyphin, apigenin, kaempferol-3-O-rutinoside, catechin, and luteolin (Ravi et al., 2017; Sahukari et al., 2021). The bioreduction mechanism begins when hydroxyl groups (R−OH) undergo oxidation to form carbonyl groups (R=O) while simultaneously reducing Ag+ to Ag0, following the reaction $Ag^+ + R{-}OH \rightarrow Ag^0 + R{-}O$ (Figure 1). As more $Ag^+$ ions are reduced, silver atoms start to aggregate, forming small clusters or nuclei. This nucleation is a crucial step where initial silver atoms congregate to form the growth seeds of nanoparticles. Once the initial silver nuclei are formed, additional silver atoms are deposited on these nuclei, leading to nanoparticle growth. Simultaneously, other phytochemicals

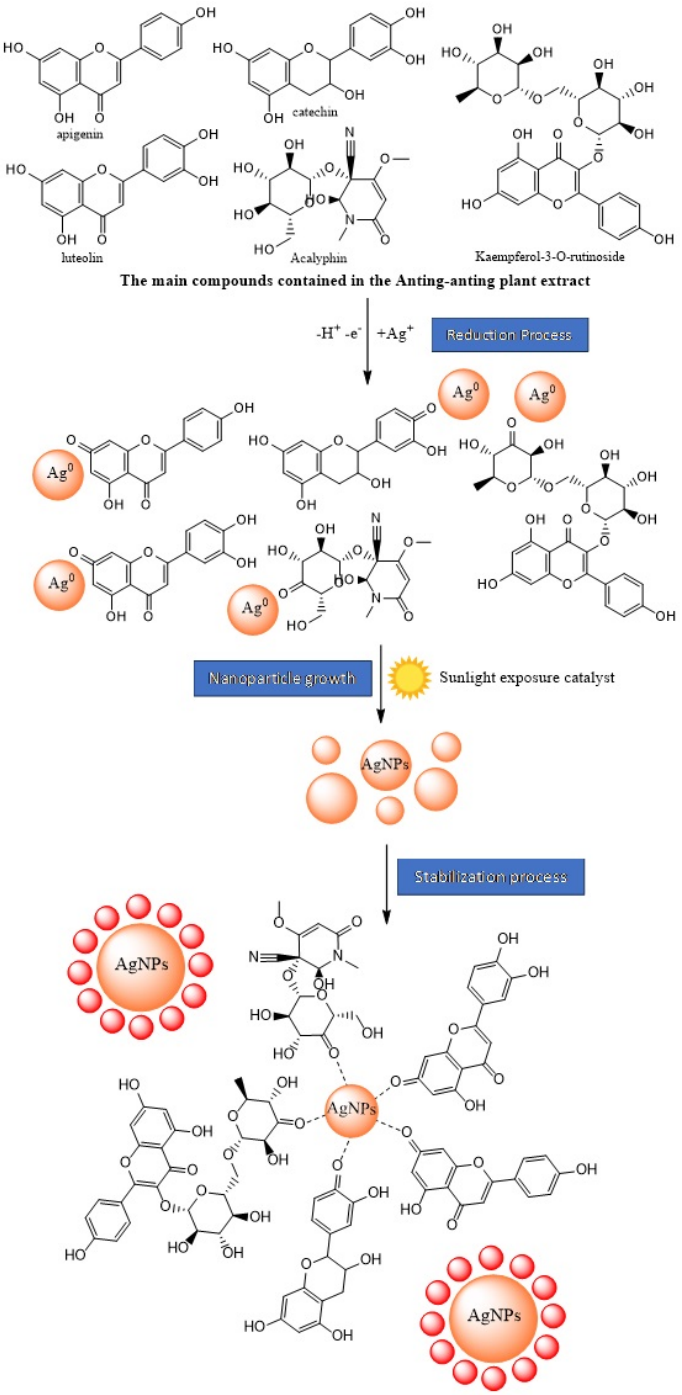


**Figure 1.** The Mechanism of AgNPs Formation and Stabilization Using Bioreductors from *Acalypha indica* L. Plant Extract

in the extract, such as proteins, flavonoids, or polysaccharides, adsorb onto the nanoparticle surfaces, stabilizing them by preventing further aggregation. This reduction and aggregation process results in the formation of SPR, which is the synchronized oscillation of electrons on the nanoparticle surface, observable as a color change in the solution, often detected using UV-Vis spectroscopy.

Sunlight irradiation in the synthesis of AgNPs acts as a catalyst to activate the active groups (Assylbekova et al., 2022) in *Acalypha indica* L. plants, facilitating the donation of electrons to silver ions ($Ag^+$) to form $Ag^0$. Although the compounds in the plant extract may degrade due to sunlight exposure, the rapid synthesis process in this work prevents significant degradation. Complex organic compounds such as flavonoids and terpenoids in the plant extract typically require weeks to months to degrade under sunlight (Chaaban et al., 2017).

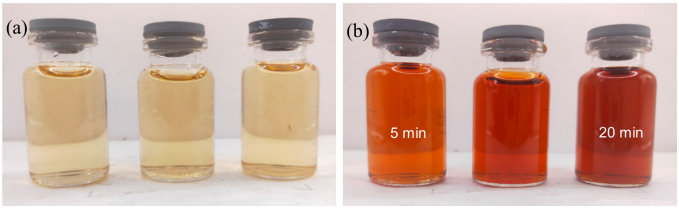


**Figure 2.** AgNPs Solution before Sunlight Exposure (a) and after Sunlight Exposure (b) for 5, 10, and 20 Minutes

The duration of exposure during AgNPs synthesis influences the nanoparticles size, shape, distribution, and stability. Insufficient exposure time results in the formation of a limited number of nanoparticles that are prone to re-oxidation. Adequate exposure time allows for optimal nanoparticle formation and growth, leading to a more homogeneous particle size distribution and higher SPR intensity. However, excessive exposure can cause agglomeration, reduced stability, and the formation of larger particles. Therefore, determining the optimal exposure time is crucial for achieving nanoparticles with the desired properties. Results depicted in Figure 2 and UV-Vis spectra in Figure 3 indicate that the optimal exposure time for AgNPs synthesis is 10 minutes, where the colloidal AgNPs are well-formed and show no signs of agglomeration. at the peak of 445 nm, the absorbance value is high at 1.987 compared to 1.393 for AgNPs at 5 minutes. In contrast, the synthesis of AgNPs for 20 minutes resulted in substantial agglomeration.

According to the UV-Vis spectral data, AgNPs display a distinct peak within the 350-500 nm wavelength range, with the most prominent peak observed at 445 nm. At an exposure time of 5 minutes, the absorbance peak of AgNPs began to form, and absorbance increased with extended exposure time up to 10 minutes, rising from 1.393 to 1.987. When the exposure time is extended to 20 minutes, the spectra display a serrated or irregular pattern. This irregular pattern in the UV-Vis spectra indicates AgNPs agglomeration, as evidenced by the presence of three peaks at 449, 440, and 425 nm, with absorbance values of 2.737, 2.737, and 2.602, respectively. The broadening of

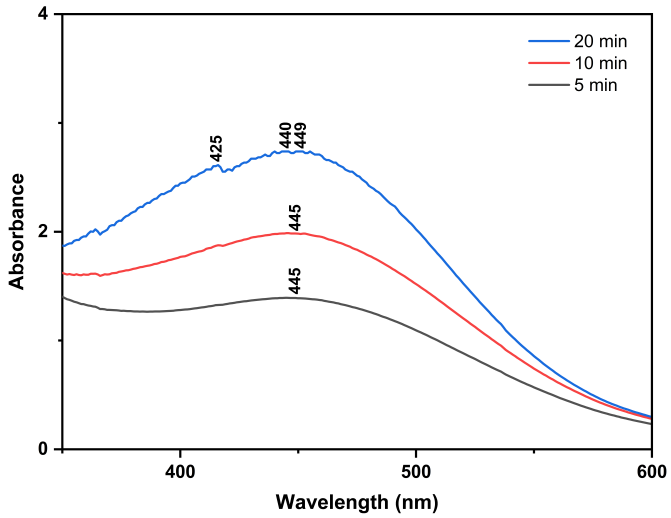


**Figure 3.** The UV-Vis Spectra of AgNPs at Different Sunlight Exposure Durations

the SPR peak, increased interparticle interactions, formation of larger aggregates, and multiple scattering events contribute to this pattern. It indicates a lack of uniformity in particle size and distribution, along with complex optical behavior due to agglomeration.

Table 1 illustrates the effect of sunlight exposure duration on the characteristics of AgNPs. At 5 minutes of exposure, the AgNPs have an average particle size of 75.59 nm with a polydispersity index (PDI) of 0.2242, suggesting a relatively homogen size distribution and a zeta potential of -22.23 mV, suggesting moderate stability. The zeta potential value is an indicator of the stability of nanoparticles (Tantra et al., 2010). With an exposure time of 10 minutes, the particle size decreases to approximately 72.8 nm, the PDI increases to 0.2196, indicating a more uniform distribution compared to the 5-minute heating, and the zeta potential rises to -23.1 mV, indicating improved stability. However, after 20 minutes of exposure, the particle size increased significantly to 227 nm, the PDI rose to 0.2519, reflecting a broader size distribution, and the zeta potential decreased to -19.49 mV, indicating reduced stability. This is due to the agglomeration of AgNPs, which results in larger particle sizes and reduced stability. The zeta potential value is an indicator of the stability of nanoparticles (Tantra et al., 2010). These findings are consistent with the UV-Vis analysis results. These results suggest that 10 minutes of sunlight exposure is optimal for producing small, uniformly distributed, and stable AgNPs, while longer exposure leads to larger, less stable particles.

### 3.2 Stability Test of AgNPs

The Table 2 shows the effects of storage time on AgNPs. On day 0, the AgNPs have a small particle size of 72.8 nm, a PDI of 0.2196 signifies a uniform and consistent size distribution, while a zeta potential of -23.10 mV indicates good stability. Af-

**Table 1.** Characteristics of AgNPs Synthesized at Varying Sunlight Exposure Durations Based on PSA Analysis

| AgNPs with Duration of Sunlight Exposure | Particle Size (nm) | Polydispersity Index | Zeta Potential (mV) |
|---|---|---|---|
| 5 min | 75.6 | 0.2242 | -22.23 |
| 10 min | 72.8 | 0.2196 | -23.10 |
| 20 min | 227 | 0.2519 | -19.49 |

**Table 2.** Storage Stability Characteristics of AgNPs Based on PSA Analysis

| AgNPs Storage Time | Particle Size (nm) | Polydispersity Index | Zeta Potential (mV) |
|---|---|---|---|
| 0 day | 72.8 | 0.2196 | -23.10 |
| 7 days | 77.2 | 0.2275 | -22.29 |
| 14 days | 108.3 | 0.3220 | -22.25 |
| 21 days | 121.2 | 0.2765 | -20.72 |
| 30 days | 193.6 | 0.2636 | -20.63 |

ter 7 days, the particle size slightly increased to 77.16 nm, with a PDI of 0.2275, still reflecting size uniformity. Although there is a slight decrease in stability with the zeta potential dropping to -22.29 mV, the AgNPs remain relatively stable. Nanoparticles with a zeta potential value below -25 mV or above +25 mV are generally considered to have high stability (Calvo et al., 1997). On day 14, the particle size grew to 108.3 nm, and the PDI rose to 0.322, signifying a broader size distribution. The zeta potential remained relatively stable at -22.25 mV, showing minimal change in stability from day 7. After extending the storage to 21 days, the particle size increased further to 121.2 nm, with a PDI of 0.2765, and the zeta potential decreased to -20.72 mV, suggesting reduced stability, though still relatively stable due to the narrow size distribution. By day 30, the particle size had grown to 193.6 nm, reflecting ongoing agglomeration of AgNPs while remaining dispersed. Although the PDI of 0.2636 indicates that the particle size distribution remains relatively uniform, the stability did not significantly differ from that observed on day 21, with a zeta potential of -20.63 mV.

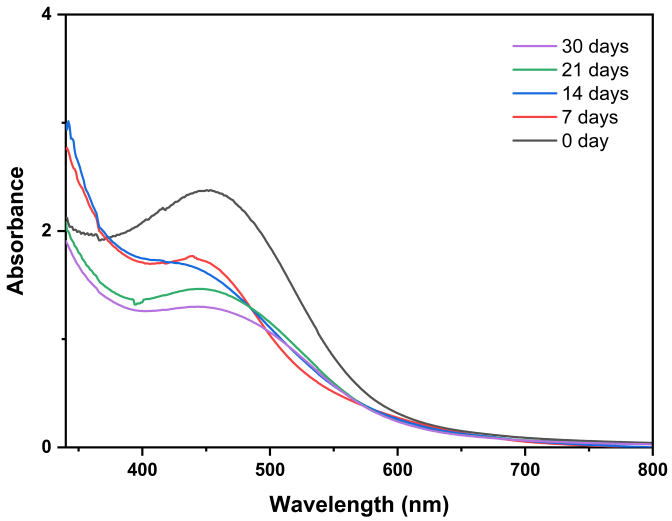


**Figure 4.** The UV-Vis Spectra of AgNPs at Different Storage Times

On the 0 day From the Figure 4, the UV-Vis spectrum displays an absorption peak near 420 nm, which is typical of AgNPs. The peak intensity is still relatively high, indicating that the nanoparticles are in a stable condition with minimal or no aggregation. By the 7$^{th}$ day, the absorption peak remains at approximately 420 nm, but there is a slight decrease in intensity. This decrease may suggest the onset of particle aggregation. On the 14$^{th}$ day, there is a possibility that the absorption peak shifts to around 425 nm, indicating potential particle size growth due to aggregation. The further decline in peak intensity suggests increased aggregation. On the 21$^{st}$ day, the absorption peak might shift further to around 430 nm, with a continuous decrease in intensity, reflecting more significant particle aggregation. By the end of the month or on the 30$^{th}$ day, the peak may shift to around 435 nm or beyond, with a significantly lower intensity, indicating a higher level of aggregation and reduced nanoparticle stability.

Changes in the size, distribution, and stability of AgNPs during storage are attributed to particle agglomeration, driven by reduced electrostatic stability, degradation of the protective layer, and potential chemical reactions such as oxidation. Over time, nanoparticles tend to coalesce into larger clusters, resulting in increased particle size, a broader size distribution, and reduced colloidal stability, as indicated by the decrease in zeta potential, the increase in particle size, and the rise in the PDI. Additionally, aggregation causes the UV-Vis absorption peak to shift to longer wavelengths (around 425 nm on day 14 and up to 435 nm on day 30) and a decrease in peak intensity. The decrease in peak intensity is due to the reduced number of individual nanoparticles interacting with UV-Vis light, reflecting a reduction in the number of nanoparticles available to absorb

light at specific wavelengths.

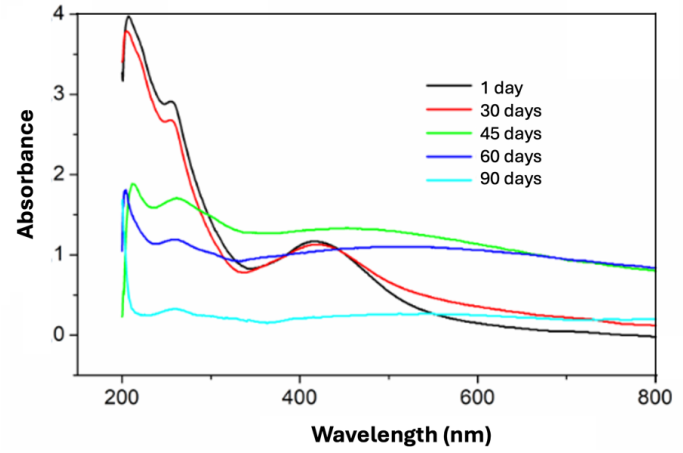


**Figure 5.** Stability of AgNPs in Phosphate-Buffered Saline (PBS) Solution

In numerous studies reported so far, AgNPs have demonstrated stability in biological and environmental media, such as Phosphate-buffered saline (PBS), when examined at 37°C. MacCuspie (2011) showed that citrate-stabilized AgNPs undergo significant agglomeration within less than an hour in PBS due to its high NaCl concentration, which reduces the repulsive forces between nanoparticles. In contrast, when AgNPs are dissolved in PBS components such as $Na_2HPO_4$ and $K_2HPO_4$, only a slight decrease in absorbance occurred over 64 hours, suggesting better stability at normal concentrations. In general, the stability of AgNPs in PBS is influenced by the high presence of NaCl, leading to rapid agglomeration, while the phosphate components of PBS do not significantly affect agglomeration at normal concentrations. In our study, AgNPs remained stable in PBS from 1 to 30 days, as indicated by a consistent spectrum, although a slight wavelength shift from 420 nm to 435 nm was observed. However, degradation of these nanoparticles occurred after 30 days of storage in PBS as shown in Figure 5. The duration of stability in PBS has also been investigated as shown in another report (Pal et al., 2016), indicating that AgNPs remain stable for more than three months. The differences in stability, as indicated by varying storage durations in PBS, is likely attributable to the different types of capping agents on the AgNPs.

The stability of AgNPs in solution is suboptimal due to rapid agglomeration caused by interactions between nanoparticles that reduce repulsive forces. In contrast, the stability of AgNPs increases significantly after the lyophilization process. This process removes water from the system, preventing the nanoparticles from being in a liquid environment that could trigger interactions such as agglomeration or coagulation. In their lyophilized form, the nanoparticles are protected from agglomeration and degradation during storage, making them more stable than AgNPs in solution. Lyophilization allows AgNPs to remain stable for a longer duration and can be reconstituted as needed without losing their functional properties. Lyophilized AgNPs demonstrate good stability, showing no significant changes in functional groups, despite a slightly wavenumber shift during storage for up to 6 months (Figure 6).

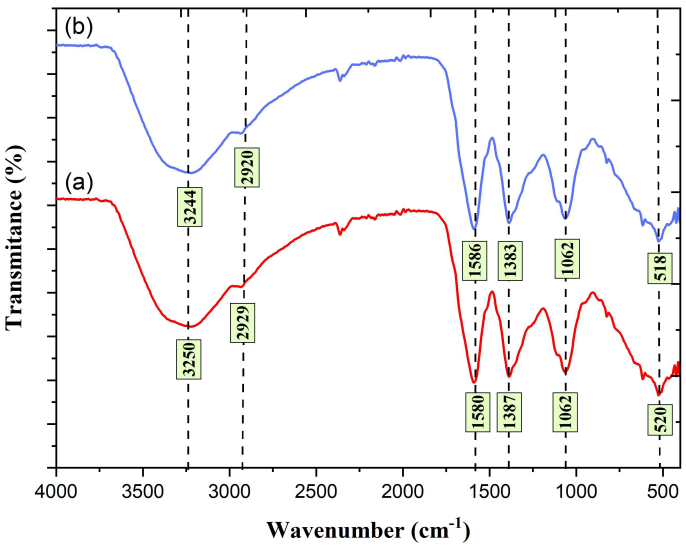


**Figure 6.** The Stability of Lyophilized Freshly Synthesized AgNPs (a) and AgNPs after 6 Months of Storage (b), Analyzed Using FTIR.

These results clearly demonstrate that AgNPs in solution undergo an increase in particle size and agglomeration over time even beyond 30 days. This is attributed to strong interparticle interactions, such as van der Waals forces, Ostwald ripening and a decrease in colloidal stability. As colloidal stability diminishes, the protective layer that maintains particle separation becomes less effective, leading to particle adhesion, aggregation, wavelength shifts, and decreased absorbance intensity in UV-Vis spectra. To maintain stability, it is essential to store AgNPs in a controlled environment with low temperatures, minimize light exposure, and regularly monitor particle size. Despite the decline in stability over time, AgNPs are still considered stable as the zeta potential remains within the ± 20 mV range. For example, even with a zeta potential around ±20 mV, particles that are small or well-dispersed can maintain stability (Muneer et al., 2023).

### 3.3 Characteristic of AgNPs Using *Acalypha indica* L. Plant Extract

The extract of *Acalypha indica* L. when compared with AgNPs shows no significant differences but does wavenumber shift as detected by FTIR (Figure 7). These shifts occur because the functional groups in the bioactive compounds within the extract are reduced and adsorbed onto the AgNPs surface (Kitimu et al., 2022). Specifically, the broad absorption peak shifts from a wavenumber of 3250 $cm^{-1}$ in the *Acalypha Indica* L. extract to 3258 $cm^{-1}$ in the AgNPs, indicating the presence of O−H

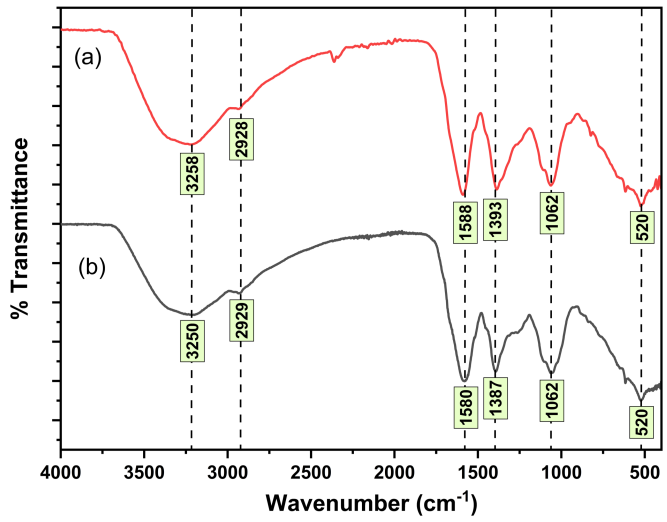


**Figure 7.** FTIR Spectra of AgNPs (a) and *Acalypha indica* L. Plant Extract (b)

groups associated with alkynes, alcohols, and phenols. Other notable peaks include 2929 $cm^{-1}$ (C−H) in the extract and 2928 $cm^{-1}$ in the AgNPs, as well as 1062 $cm^{-1}$ (C−O) in both. The wavenumber of 1580 $cm^{-1}$, which signifies N−H bending of flavonoids, is observed in the *Acalypha indica* L. extract and shifts to 1588 $cm^{-1}$ in the AgNPs. The nitro group (N=O bend) appears at 1393 $cm^{-1}$ in the extract and 1387 $cm^{-1}$ in the AgNPs, while the alkyl halide peak is found at 520 $cm^{-1}$ in both samples. The organic compounds, such as flavonoids or alkaloids, in the extract are likely involved in the synthesis of AgNPs, and proteins present in the extract may contribute to stabilizing the surrounding AgNPs.

Based on the morphological analysis of AgNPs synthesized using the plant bioreductor *Acalypha indica* L., as observed through TEM (Figure 8), the nanoparticles are spherical with an average size of approximately 7.13 nm. Their sizes range from 3 to 15 nm, the most frequently observed sizes between 5 and 6 nm.

### 3.4 Anticancer Activity Test of AgNPs

Cell viability assays are essential for evaluating cellular responses to toxic substances, including aspects of cell survival, death, and metabolic function. In this research, the MTT assay was utilized to assess the cytotoxicity of AgNPs. Each treatment was administered at various concentrations (400, 200, 100, 50, and 25 $\mu$g/mL) of lyophilized AgNPs and incubated with the cells for 24 hours to assess whether these treatments affected cancer cell viability. The $IC_{50}$ of the AgNPs was found to be approximately 261.21 $\mu$g/mL, as illustrated by the graph plotting cell viability (Y-axis) against concentration (X-axis) ranging from 0 to 400 $\mu$g/mL (Figure 9). The MTT assay further validated the dose and time-dependent cytotoxic effects of AgNPs on the T47D cell line (Table 3).

The efficacy of AgNPs as anticancer agents is highlighted

**Table 3.** The Dose-Dependent Cytotoxic Effects of AgNPs on the T47D Cell Line for 24 Hours

| Lyophilized AgNPs Concentration ($\mu$g/mL) | Cell Viability (%) |
|---|---|
| 400 | 13.72 |
| 200 | 73.96 |
| 100 | 91.66 |
| 50 | 92.85 |
| 25 | 93.37 |
| Control*1 | 100 |

*1 Cells without AgNPs treatment

by their capacity to suppress cancer cell proliferation through mechanisms such as inducing oxidative stress and causing cellular damage, leading to apoptosis. Apoptosis, a mechanism of programmed cell death designed to systematically remove damaged or dysfunctional cells, can be triggered through both mitochondria-dependent and mitochondria-independent pathways, potentially leading to the inhibition of T47D cell proliferation (Abass Sofi et al., 2022; Alkan et al., 2022; Farah et al., 2016). Apoptosis, a mechanism of programmed cell death designed to systematically remove damaged or dysfunctional cells, can be triggered through both mitochondria-dependent and mitochondria-independent pathways, potentially leading to the inhibition of T47D cell proliferation (Jeyaraj et al., 2015). Although the $IC_{50}$ values reflect the potency of AgNPs alone, the presence of bioactive compounds from the aqueous leaf extract of *Acalypha indica* L. plays a synergistic role. These compounds contribute to the synthesis of AgNPs and enhance their anticancer effects by working in tandem with the nanoparticles. The combined action of AgNPs and the bioactive components from the extract suggests that both elements are crucial in targeting and disrupting key processes involved in cancer cell proliferation. This synergy underscores the promising potential of AgNPs, both through their intrinsic properties and the contribution of plant-derived compounds, in developing effective cancer therapies.

The safety of AgNPs as therapeutic agents has been assessed in various studies using hemolysis assays on healthy cells, particularly red blood cells (RBCs). These studies indicate that the toxicity of AgNPs to healthy cells depends on factors such as concentration and exposure duration, with prolonged or high concentrations potentially leading to hemolysis or cytotoxic effects. Particle size, shape, surface properties, and concentration are critical in determining this response, as higher concentrations increase interactions with cell membranes, triggering immune responses and producing reactive oxygen species (ROS), which cause oxidative stress and cell death (Huang et al., 2016; Rujanapun et al., 2015). However, AgNPs synthesized using plant extracts tend to be safer for RBCs compared to positive controls like Triton-X, which induces 100% hemolysis (Liaqat et al., 2022), and we suppose that the AgNPs synthesized in our work also have similar properties for RBCs. This

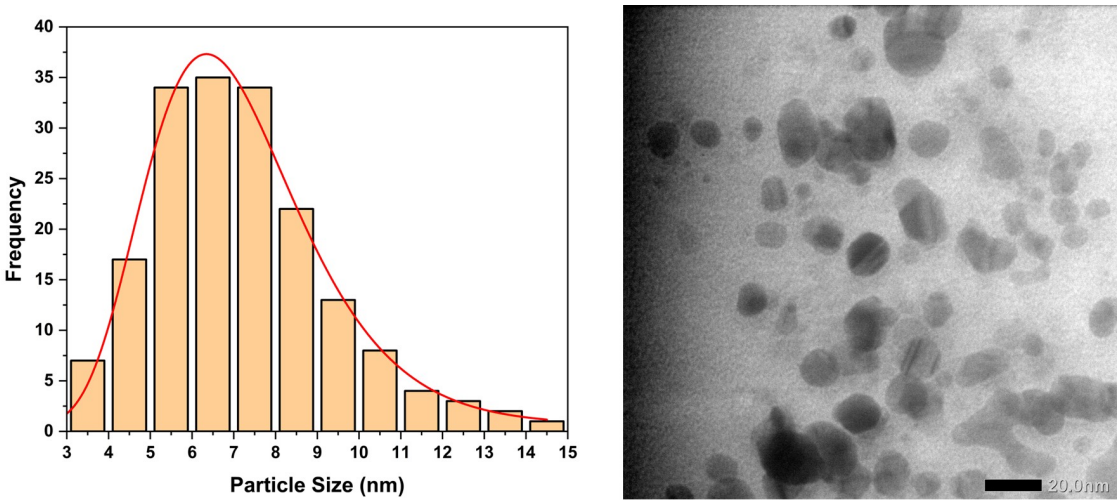


**Figure 8.** Analysis of Shape and Size Distribution of Nanoparticles Based on TEM Image

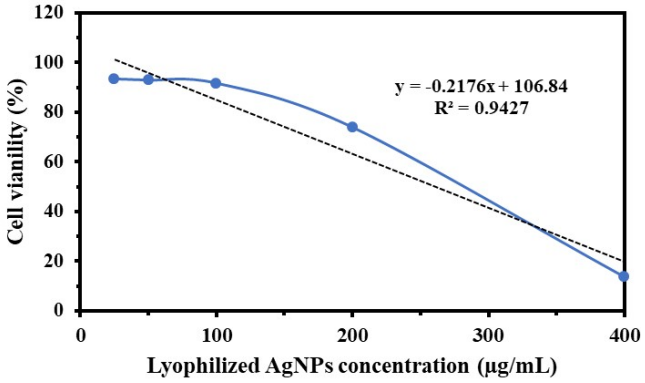


**Figure 9.** The Viability of T47D Cells after 24 Hours of AgNPs Treatment for $IC_{50}$ Estimation

enhanced safety is attributed to bioactive components in plant extracts, such as flavonoids and polyphenols, that act as natural stabilizing agents, forming a protective layer around the nanoparticles, thereby reducing their direct interaction with cell membranes. Additionally, biologically synthesized AgNPs tend to have smaller particle sizes and more uniform distribution, which lowers the risk of cell damage, while the antioxidant properties of the plant extracts help alleviate oxidative stress (Bian et al., 2019; Chen et al., 2015).

## 4. CONCLUSIONS

This study provides a comprehensive evaluation of the stability and anticancer potential of AgNPs synthesized using *Acalypha indica* L. extract. The findings indicate that AgNPs in a dispersed solution experience a decrease in absorbance intensity over time due to particle agglomeration, leading to an increase in particle size and a decline in zeta potential stability. However, the AgNPs remained stable for up to 30 days, with the zeta potential showing no significant decrease and remaining within the ±20 mV range. The silver nanoparticles also maintained a homogeneous size, as reflected by the PDI values indicating uniformity. The optimal sunlight exposure time was found to be 10 minutes, during which high absorbance was achieved, effectively preserving structural integrity and therapeutic efficacy. The AgNPs also demonstrated significant cytotoxic effects against T47D breast cancer cells, highlighting their potential as effective anticancer agents. To ensure long-term stability and efficacy, further optimization is required, including the use of stabilizing agents or modifications to the nanoparticle formulation. Overall, while AgNPs synthesized from *Acalypha indica* L. show substantial promise for cancer therapy, ongoing refinement is crucial to enhance their stability and therapeutic performance.

## 5. ACKNOWLEDGMENT

We extend our gratitude to the Directorate of Research and Community Service, Brawijaya University, for their financial support through the Flagship Basic Research Grant, No: 00140.11/UN10.A0501/B/PT.01.03.2/2024. We also wish to thank Prof. Widodo, Ph.D., Med.Sc. of Brawijaya University for providing the T47D breast cancer cells.

## REFERENCES

Abass Sofi, M., S. Sunitha, M. Ashaq Sofi, S. K. Khadheer Pasha, and D. Choi (2022). An Overview of Antimicrobial and Anticancer Potential of Silver Nanoparticles. *Journal of King Saud University - Science*, **34**(2); 101791

Alkan, H., I. H. Cigerci, M. M. Ali, O. Hazman, R. Liman, F. Cola, and E. Bonciu (2022). Cytotoxic and Genotoxic Evaluation of Biosynthesized Silver Nanoparticles Using Moringa Oleifera on MCF-7 and HUVEC Cell Lines. *Plants*, **11**(10); 1293

Assylbekova, G., H. F. Alotaibi, S. Yegemberdiyeva, A. Suigen-

 

bayeva, M. Sataev, S. Koshkarbaeva, P. Abdurazova, S. Sakibayeva, and P. Prokopovich (2022). Sunlight Induced Synthesis of Silver Nanoparticles on Cellulose for the Preparation of Antimicrobial Textiles. *Journal of Photochemistry and Photobiology*, **11**; 100134

Aziz, N., M. Faraz, M. A. Sherwani, T. Fatma, and R. Prasad (2019). Illuminating the Anticancerous Efficacy of a New Fungal Chassis for Silver Nanoparticle Synthesis. *Frontiers in Chemistry*, **7**(6); 5

Basak, P., R. Majumder, A. Jasu, S. Paul, and S. Biswas (2018). Potential Therapeutic Activity of Bio-Synthesized Silver Nanoparticles as Anticancer and Antimicrobial Agent. *IOP Conference Series: Materials Science and Engineering*, **410**; 012020

Belzile-Dugas, E. and M. J. Eisenberg (2021). Radiation-Induced Cardiovascular Disease: Review of an Underrecognized Pathology. *Journal of the American Heart Association*, **10**(18); e021686

Bian, Y., K. Kim, T. Ngo, I. Kim, O. Bae, K. Lim, and J. Chung (2019). Silver Nanoparticles Promote Procoagulant Activity of Red Blood Cells: A Potential Risk of Thrombosis in Susceptible Population. *Particle and Fibre Toxicology*, **16**(1); 9

Calcaterra, I., G. Iannuzzo, F. Dell'Aquila, and M. N. D. Di Minno (2020). Pathophysiological Role of Synovitis in Hemophilic Arthropathy Development: A Two-Hit Hypothesis. *Frontiers in Physiology*, **11**; 541

Calvo, P., C. Remunan-Lopez, J. L. Vila-Jato, and M. J. Alonso (1997). Novel Hydrophilic Chitosan-Polyethylene Oxide Nanoparticles as Protein Carriers. *Journal of Applied Polymer Science*, **63**(1); 125–132

Chaaban, H., I. Ioannou, C. Paris, C. Charbonnel, and M. Ghoul (2017). The Photostability of Flavanones, Flavonols and Flavones and Evolution of Their Antioxidant Activity. *Journal of Photochemistry and Photobiology A: Chemistry*, **336**; 131–139

Chen, L. Q., L. Fang, J. Ling, C. Z. Ding, B. Kang, and C. Z. Huang (2015). Nanotoxicity of Silver Nanoparticles to Red Blood Cells: Size Dependent Adsorption, Uptake, and Hemolytic Activity. *Chemical Research in Toxicology*, **28**(3); 501–509

Chen, X. and H. J. Schluesener (2008). Nanosilver: A Nanoproduct in Medical Application. *Toxicology Letters*, **176**(1); 1–12

Chouhan, N. (2018). Silver Nanoparticles: Synthesis, Characterization and Applications. In *Silver Nanoparticles - Fabrication, Characterization and Applications*. InTech

Dzoyem, J. P., R. T. Tchuenguem, J. Iqbal, M. A. Yameen, A. Mannan, I. Shahzadi, T. Ismail, N. Fatima, and G. Murtaza (2022). Anticandidal Activity of Green Synthesised Silver Nanoparticles and Extract Loaded Chitosan Nanoparticles of *Euphorbia prostata*. *Artificial Cells, Nanomedicine, and Biotechnology*, **50**(1); 188–197

El-Refai, A. A., G. Ghoniem, A. Y. El-Khateeb, and M. M. Hassaan (2018). Cytotoxicity of Aqueous Garlic and Ginger Metal Nanoparticles Extracts against Tumor Cell Lines "In Vitro". *Journal of Food and Dairy Sciences*, **9**(2); 51–58

Farah, M. A., M. A. Ali, S. Chen, Y. Li, F. M. Al-Hemaid, F. M. Abou-Tarboush, K. M. Al-Anazi, and J. Lee (2016). Silver nanoparticles synthesized from Adenium obesum leaf extract induced DNA damage, apoptosis and autophagy via generation of reactive oxygen species. *Colloids and Surfaces B: Biointerfaces*, **141**; 158–169

Felimban, A. I., N. S. Alharbi, and N. S. Alsubhi (2022). Optimization, Characterization, and Anticancer Potential of Silver Nanoparticles Biosynthesized Using *Olea europaea*. *International Journal of Biomaterials*, **1**; 6859637

Fiddaroini, S., K. Indu, S. Amalia, I. O. Wulandari, A. Mulyasuryani, L. Dinira, and A. Sabarudin (2023). Cottonwood Honey (*Ceiba pentandra*) as Bioreductor for Preparation of AgNPs-mediated Chitosan-based Hand Gel Sanitizer. *Tropical Journal of Natural Product Research*, **7**(12); 5573–5580

Guilger-Casagrande, M. and R. d. Lima (2019). Synthesis of Silver Nanoparticles Mediated by Fungi: A Review. *Frontiers in Bioengineering and Biotechnology*, **7**; 128

Hamad, M. T. (2019). Biosynthesis of Silver Nanoparticles by Fungi and Their Antibacterial Activity. *International Journal of Environmental Science and Technology*, **16**(2); 1015–1024

Heidari, Z., A. Salehzadeh, S. A. Sadat Shandiz, and S. Tajdoost (2018). Anti-Cancer and Anti-Oxidant Properties of Ethanolic Leaf Extract of *Thymus vulgaris* and Its Bio-Functionalized Silver Nanoparticles. *3 Biotech*, **8**(3); 177

Huang, H., W. Lai, M. Cui, L. Liang, Y. Lin, Q. Fang, Y. Liu, and L. Xie (2016). An Evaluation of Blood Compatibility of Silver Nanoparticles. *Scientific Reports*, **6**(1); 25518

Ibrahim, E., H. Fouad, M. Zhang, Y. Zhang, W. Qiu, C. Yan, B. Li, J. Mo, and J. Chen (2019). Biosynthesis of Silver Nanoparticles Using Endophytic Bacteria and Their Role in Inhibition of Rice Pathogenic Bacteria and Plant Growth Promotion. *RSC Advances*, **9**(50); 29293–29299

Jeyaraj, M., A. Renganathan, G. Sathishkumar, A. Ganapathi, and K. Premkumar (2015). Biogenic Metal Nanoformulations Induce Bax/$Bcl_2$ and Caspase Mediated Mitochondrial Dysfunction in Human Breast Cancer Cells (mcf 7). *RSC Advances*, **5**(3); 2159–2166

Kitimu, S., P. Kirira, and J. Sokei (2022). Biogenic Synthesis of Silver Nanoparticles Using *Azadirachta indica* Methanolic Bark Extract and Their Anti-Proliferative Activities against DU-145 Human Prostate Cancer Cells. *African Journal of Biotechnology*, **2**; 64–72

Lava, M. B., U. M. Muddapur, N. Basavegowda, S. S. More, and V. S. More (2021). Characterization, Anticancer, Antibacterial, Anti-Diabetic and Anti-Inflammatory Activities of Green Synthesized Silver Nanoparticles Using Justica Wynaadensis Leaves Extract. *Materials Today: Proceedings*, **46**; 5942–5947

Liaqat, N., N. Jahan, K. ur Rahman, T. Anwar, and H. Qureshi (2022). Green Synthesized Silver Nanoparticles: Optimization, Characterization, Antimicrobial Activity, and Cytotoxicity Study by Hemolysis Assay. *Frontiers in Chemistry*, **10**;

 

952006
MacCuspie, R. I. (2011). Colloidal Stability of Silver Nanoparticles in Biologically Relevant Conditions. *Journal of Nanoparticle Research*, **13**(7); 2893–2908
Mousavi, B., F. Tafvizi, and S. Zaker Bostanabad (2018). Green Synthesis of Silver Nanoparticles Using *Artemisia turcomanica* Leaf Extract and the Study of Anti-Cancer Effect and Apoptosis Induction on Gastric Cancer Cell Line (ags). *Artificial Cells, Nanomedicine, and Biotechnology*, **46**(sup1); 499–510
Muneer, R., M. R. Hashmet, P. Pourafshary, and M. Shakeel (2023). Unlocking the Power of Artificial Intelligence: Accurate Zeta Potential Prediction Using Machine Learning. *Nanomaterials*, **13**(7); 1209
Murugesan, A. K., B. Pannerselvam, A. Javee, M. Rajenderan, and D. Thiyagarajan (2021). Facile Green Synthesis and Characterization of *Gloriosa superba* L. Tuber Extract-Capped Silver Nanoparticles (GST-AgNPs) and Its Potential Antibacterial and Anticancer Activities Against A549 Human Cancer Cells. *Environmental Nanotechnology, Monitoring & Management*, **15**; 100460
Naveenkumar, S., C. Kamaraj, C. Ragavendran, M. Vaithiyalingam, V. Sugumar, and K. Marimuthu (2023). Gracilaria Corticata Red Seaweed Mediate Biosynthesis of Silver Nanoparticles: Larvicidal, Neurotoxicity, Molecular Docking Analysis, and Ecofriendly Approach. *Biomass Conversion and Biorefinery*, **14**(17); 20567–20609
Nindrea, R. D., I. Dwiprahasto, L. Lazuardi, and T. Aryandono (2023). Development of a Breast Cancer Risk Screening Tool for Women in Indonesia. *Clinical Epidemiology and Global Health*, **24**; 101446
Oves, M., M. Ahmar Rauf, M. Aslam, H. A. Qari, H. Sonbol, I. Ahmad, G. Sarwar Zaman, and M. Saeed (2022). Green Synthesis of Silver Nanoparticles by *Conocarpus lancifolius* Plant Extract and Their Antimicrobial and Anticancer Activities. *Saudi Journal of Biological Sciences*, **29**(1); 460–471
Pal, I., V. P. Brahmkhatri, S. Bera, D. Bhattacharyya, Y. Quirishi, A. Bhunia, and H. S. Atreya (2016). Enhanced Stability and Activity of an Antimicrobial Peptide in Conjugation with Silver Nanoparticle. *Journal of Colloid and Interface Science*, **483**; 385–393
Rahman, M. F., A. Aulanni, A. Sabarudin, S. M. Ulfa, E. Setiawan, and M. Masruri (2023). Metabolites Analysis of the Marine Sponge *Callyspongia affinis* from Kangean Island as a Potential Source for Anticancer Candidates. *Journal of Applied Pharmaceutical Science*, **13**(5); 136–143
Rahman, M. F., M. N. Haykal, N. A. Siagian, P. M. Sriepindonnta, and N. A. Tampubolon (2018). Synthesis and Proapoptotic Activity on Cervical Cancer Cell of Ester Eugenol 1-(3-Methoxy-4-hydroxy)phenyl-2-propylmethanoate. *IOP Conference Series: Materials Science and Engineering*, **299**; 012071
Ravi, S., B. Shanmugam, G. V. Subbaiah, S. H. Prasad, and K. S. Reddy (2017). Identification of Food Preservative, Stress Relief Compounds by GC–MS and HR-LC/Q-TOF/MS; Evaluation of Antioxidant Activity of *Acalypha indica* Leaves Methanolic Extract (In Vitro) and Polyphenolic Fraction (In Vivo). *Journal of Food Science and Technology*, **54**(6); 1585–1596
Rujanapun, N., S. Aueviriyavit, S. Boonrungsiman, A. Rosena, D. Phummiratch, S. Riolueang, N. Chalaow, V. Viprakasit, and R. Maniratanachote (2015). Human Primary Erythroid Cells as a More Sensitive Alternative In Vitro Hematological Model for Nanotoxicity Studies: Toxicological Effects of Silver Nanoparticles. *Toxicology in Vitro*, **29**(8); 1982–1992
Sahukari, R., J. Punabaka, S. Bhasha, V. S. Ganjikunta, S. Kondeti Ramudu, S. R. Kesireddy, W. Ye, and M. Korivi (2021). Phytochemical Profile, Free Radical Scavenging and Anti-Inflammatory Properties of *Acalypha indica* Root Extract: Evidence from In Vitro and In Vivo Studies. *Molecules*, **26**(20); 6251
Siegel, R. L., A. N. Giaquinto, and A. Jemal (2024). Cancer Statistics. *CA: A Cancer Journal for Clinicians*, **74**(1); 12–49
Sritharan, S. and N. Sivalingam (2021). A Comprehensive Review on Time-Tested Anticancer Drug Doxorubicin. *Life Sciences*, **278**; 119527
Sung, H., J. Ferlay, R. L. Siegel, M. Laversanne, I. Soerjomataram, A. Jemal, and F. Bray (2021). Global Cancer Statistics 2020: GLOBOCAN Estimates of Incidence and Mortality Worldwide for 36 Cancers in 185 Countries. *CA: A Cancer Journal for Clinicians*, **71**(3); 209–249
Tantra, R., P. Schulze, and P. Quincey (2010). Effect of Nanoparticle Concentration on Zeta-Potential Measurement Results and Reproducibility. *Particuology*, **8**(3); 279–285
World Health Organization (2020). *WHO Methods and Data Sources for Country-level Causes of Death 2000-2019*. World Health Organization
Wulandari, I. O., B. E. Pebriatin, V. Valiana, S. Hadisaputra, A. D. Ananto, and A. Sabarudin (2022). Green Synthesis of Silver Nanoparticles Coated by Water Soluble Chitosan and Its Potency as Non-Alcoholic Hand Sanitizer Formulation. *Materials*, **15**(13); 4641
Xu, L., Y.-Y. Wang, J. Huang, C. Chen, Z. Wang, and H. Xie (2020). Silver Nanoparticles: Synthesis, Medical Applications and Biosafety. *Theranostics*, **10**(20); 8996–9031
Yesilot, S. and C. Aydın Acar (2019). Silver Nanoparticles; A New Hope in Cancer Therapy? *Eastern Journal Of Medicine*, **24**(1); 111–116
Yoon, K., J. Hoon Byeon, J. Park, and J. Hwang (2007). Susceptibility Constants of *Escherichia coli* and *Bacillus subtilis* to Silver and Copper Nanoparticles. *Science of The Total Environment*, **373**(2–3); 572–575

 